Using Polynomials to Correct Non-uniform Backgrounds in Thermal Images Caused by Uneven Heating

Kai-Yi Zheng[1] Yu-Sung Chang Kai-Hong Wang Yuan Yao[2*]
Department of Chemical Engineering, National Tsing Hua University, Hsinchu, Taiwan
[1]beihai722@126.com
[2*]Corresponding author, yyao@mx.nthu.edu. tw

Abstract

In order to correct non-uniform backgrounds in thermal images of carbon fiber-reinforced polymers (CFRP), we propose a processing and analysis procedure in this paper. We apply thermographic signal reconstruction (TSR) using time-direction information to reduce noise in thermal images, followed by Whittaker smoothing (WS) to further reduce noise in two-dimensional image space. Finally, polynomial background correction (PBC) is used to correct non-uniform backgrounds retained in the reconstructed thermal images. We tested a CFRP specimen with seven defective regions using the proposed method. The results showed that with the aid of PBC, the non-uniform background caused by uneven heating was successfully corrected and the defective regions were easily identified.

1. Introduction

Carbon fiber-reinforced polymer (CFRP) is a widely used material in aerospace, automotive, civil engineering, etc., which has several advantages, such as low density, high chemical stability, and high mechanical strength. However, it is susceptible to defects, including cracks, delamination, debonding, and void formation in carbon fiber, due to operation errors in manufacturing. Thus, testing and identifying the defects of CFRP in time is necessary during manufacture [1-3]. Due to the high cost of CFRP, pulsed thermography (PT) as a non-destructive testing (NDT) method is commonly used, and has the advantages of a wide scanning scope as well as easy and safe operation.

In PT, due to noise and non-uniform backgrounds caused by uneven heating, it is necessary to use methods of numerical analysis to enhance signals after obtaining the thermal images. Hence, a few methods have been proposed to process thermal images based on Fourier diffusion equations, such as thermographic signal reconstruction (TSR) [4-6], differential absolute contrast (DAC) [7], and pulsed-phase thermography (PPT) [8] etc. Of these methods, TSR has exhibited superior performance in reducing noise and enhancing signals in defective regions. However, TSR uses polynomials to reduce noise only through time direction, but not in a two-dimensional (2D) image space. Furthermore, the non-uniform background caused by uneven heating cannot be adequately corrected because polynomial fitting is only an approximate solution of the Fourier diffusion equation. Hence, thermal images pretreated by TSR should be further treated in 2D image space.

Each thermal image consists of vectors in both rows and columns. Thus, correcting the background of an image can be treated as correcting the baseline of each vector. The polynomial function can also be used to construct the baseline of signals in an adaptive manner. Hence, in this paper, we construct the backgrounds of thermal images using the method of polynomial background correction (PBC), and thus eliminate them from the original thermographic signal [9].

2. Algorithms

2.1 Thermographic signal reconstruction

Based on the Fourier diffusion equation, the problem of heat diffusion through a solid specimen can be expressed as follows:

$$T(z,t) = T_0 + \frac{Q}{e\sqrt{\pi t}} \exp\left(-\frac{z^2}{4\alpha t}\right) \qquad (1)$$

where T_0 is the ambient temperature, Q is the energy of the pulse from flash light, z the depth of the CFRP sheet, t the time after the pulse, and e and α are both parameters related to the property of the material. Since thermal images can only capture the surface temperature of CFRP, z is set to zero. Setting $T(t,0) - T_0$ as ΔT, Equation (1) can be modified as

$$\Delta T = \frac{Q}{e\sqrt{\pi t}} \qquad (2)$$

Taking the logarithm on both sides of Equation (2), the linear model between ΔT and t can be expressed as Equation (3):

$$ln(\Delta T) = ln\frac{Q}{ae\sqrt{\pi}} - 0.5lnt \qquad (3)$$

Equation (3) is concise, but it is only an approximate solution of the Fourier diffusion equation. Thus, the real thermographic data may diverge from the ideal linear equation expressed as Equation (3). In order to solve this problem, the linear model should be modified to a polynomial function of degree n:

$$ln(\Delta T) = a_0 + a_1 (\ln t)^1 + \cdots + a_n (\ln t)^m \qquad (4)$$

In Equation (4), an excessively large value of m may extract too much noise. Because of this, the value of m is usually set to 4. For a CFRP specimen, the declining curves of temperature corresponding to defective regions behave differently from those of intact regions [4]. Since the heat transfer coefficients in the defective regions are smaller than that of carbon fiber, at each fixed time point, the temperature values in the defective regions (e.g., regions containing Teflon or other defects) are higher than those in intact regions. Therefore, at each time point, the difference in temperature values between defective and intact regions reflect the positions of the defective regions.

2.2 Polynomial background correction

In this paper, we pretreat the original thermal images by TSR and Whittaker smoothing (WS) [11] in order to reduce noise. Following this, PBC is applied to correct the non-uniform background contained in the reconstructed images.

Because of each thermal image composed of vectors in both column and row directions, the background correction can be executed by the vectors. Thus, in this paper, PBC is applied to pretreat each row of image for correcting the background in row direction at first. Then, each column of image is corrected by PBC. The algorithm of PBC can be shown as follows:

For each row or column in a reconstructed thermal image, a vector ($\boldsymbol{y}$) can be fitted using a polynomial function with n degree [9]:

$$\begin{bmatrix} 1 & x_1 & \cdots & x_1^n \\ 1 & x_2 & \cdots & x_2^n \\ \cdots & \cdots & \cdots & \cdots \\ 1 & x_m & \cdots & x_m^n \end{bmatrix} \begin{bmatrix} a_0 \\ a_1 \\ a_2 \\ \cdots \\ a_n \end{bmatrix} = \begin{bmatrix} y_1 \\ y_2 \\ \cdots \\ y_m \end{bmatrix} \tag{5}$$

In Equation (5), x_1, $x_2 \ldots x_m$ can be considered to be integers from 1 to m, and a_1, $a_2 \ldots a_n$ as the corresponding polynomial coefficients. Thus, Equation (5) can be rewritten in the matrix form

$$\boldsymbol{Xa} = \boldsymbol{y} \tag{6}$$

and $\boldsymbol{a}$ can be estimated as

$$\hat{\boldsymbol{a}} = (\boldsymbol{X}'\boldsymbol{X})^{-1}\boldsymbol{X}'\boldsymbol{y} \tag{7}$$

The estimated values of y can be shown as follows:

$$\hat{\boldsymbol{y}} = \boldsymbol{X}\hat{\boldsymbol{a}} = \boldsymbol{X}(\boldsymbol{X}'\boldsymbol{X})^{-1}\boldsymbol{X}'\boldsymbol{y} \tag{8}$$

Based on the methods of fitting polynomials, the algorithm for PBC can be executed in the following steps [9]:

(1) Set the original signal as $\boldsymbol{y}_0$, and set the power of the polynomial function to (n).
(2) Compute the fitted signals $\boldsymbol{b}$ from $\boldsymbol{y}_{k-1}$ by Equation (8) in the k-th iteration.
(3) Compare $\boldsymbol{b}$ and $\boldsymbol{y}_{k-1}$, and choose the smaller value in each pair of elements to construct a new signal $\boldsymbol{y}_k$.
(4) Repeated Steps (2)-(4), until Equation (9) is obtained.
(5) The fitted vector can be seen as the background of the signal to be removed.

$$\left\| \frac{\boldsymbol{y}_{k-1} - \boldsymbol{y}_k}{\boldsymbol{y}_{k-1}} \right\| < 0.001 \tag{9}$$

To determine the effects of pretreatment, the signal-to-noise ratio (SNR) of the resulting image is computed as follows:

$$\text{SNR} = \frac{M_{def} - M_{in}}{\sigma_{in}} \tag{10}$$

In Equation (10), M_{def} denotes the mean intensity of the defective regions, M_{in} the mean intensity of intact regions, and σ_{in} the standard deviation of the intensity of the intact regions. The SNR can, of course, be improved by raising the intensity divergence between the defective and intact regions, and reducing the variation among the intact regions [4, 10].

3. Experiment results

In experiments, we produced a CFRP specimen by vacuum-assisted resin transfer molding (VARTM) [12, 13]. Teflon sheets were inserted in six regions with different areas and depths in order to simulate defective regions. Furthermore, another defective region was constructed at the top-left of the CFRP. The specimen is shown in Figure 1.

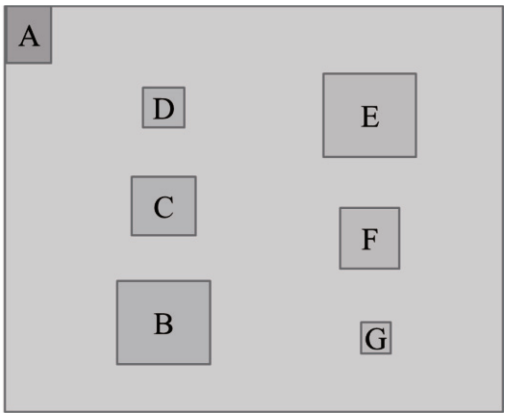

Figure 1. CFRP specimen with defective regions

In Figure 1, Region A is a randomly generated defective region. The defects in Regions B, C, and D are each under a single layer of a sheet of carbon fiber of widths 1.6 cm, 0.8 cm, and 0.4 cm, respectively, while the defects in Regions E, F, and G are under double layers of carbon fiber sheets.

After constructing the CFRP specimen, PT was executed. Following pulsed heating, thermographic data collection was carried out using a NEC TAS-G100EXD thermal camera. The termination time of the image capture was 12 s after the pulse, and 180 pieces of thermal images were obtained. TSR, WS, and PBC were then executed for noise reduction and background elimination.

4. Results and Discussion

The thermal images at 1, 2, 3 and 4 s without and with pretreatment by TSR are shown in Figures 2 and 3, respectively.

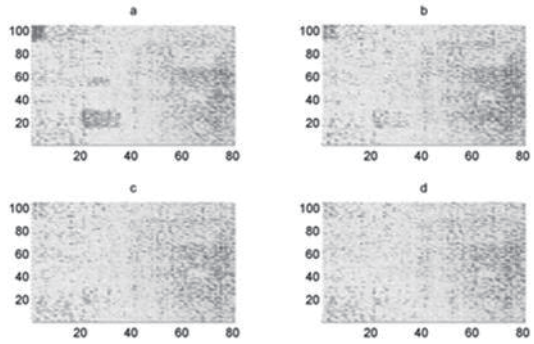

Figure 2. The original thermal images of CFRP specimen at (a) t = 1 s, (b) t = 2 s, (c) t = 3 s, and (d) t = 4 s

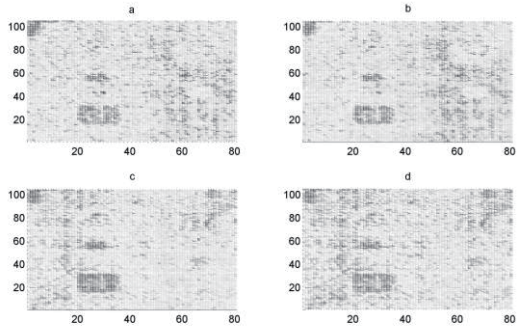

Figure 3. The thermal images at (a) t = 1 s, (b) t = 2 s, (c) t = 3 s, and (d) t = 4 s after TSR

Compared to Figure 2, it is obvious that with the help of TSR, the intensities of the defective regions in Figure 3 were significantly enhanced, especially for thermal images at t = 3 s and 4 s. This is because TSR can reduce noise. However, noise in each reconstructed image was still quite significant. Therefore, the noise needs further pretreatment in 2D image space using WS. The results are shown in Figure 4.

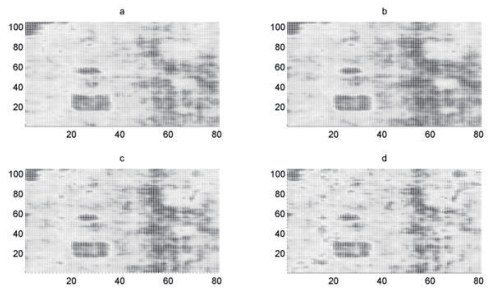

Figure 4. Thermal images at (a) t = 1 s, (b) t = 2 s, (c) t = 3 s, (d) t = 4 s after TSR and WS

Figure 4 shows that the noise in the images was largely removed. However, non-uniform backgrounds still exist. Thus, PBC should be used. The results are shown in Figure 5.

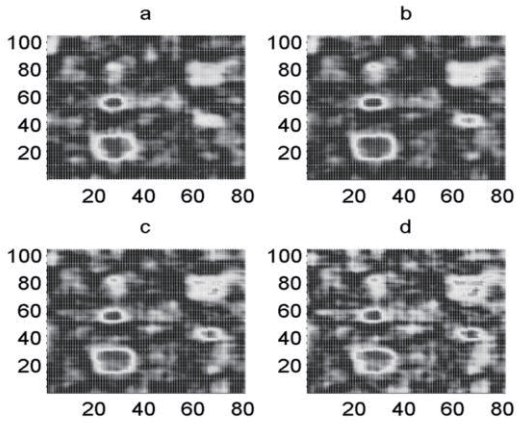

Figure 5. The thermal images at (a) t = 1 s, (b) t = 2 s, (c) t = 3 s, and (d) t = 4 s after TSR, WS, and PBC

In each image in Figure 5, the background due to uneven heating was successfully eliminated. Hence, the defective regions A, B, C, D, E, F, and G were all easily recognized. Such results verify the effectiveness of our proposed method.

Furthermore, the SNR of all 180 thermal images were calculated after using different pretreatment methods. The results are shown in Figure 6.

From Figure 6, it is obvious that at each time point, images without any pretreatment have the lowest SNR values. TSR and WS can enhance SNR by noise reduction. After correcting the background using PBC, the SNR has the highest values, nearly two times of that by TSR and WS. This further confirms that PBC-based background elimination is effective.

5. Conclusions

For defect detection in CFRP products, PT is a widely used method. However, existing thermal image processing methods have certain limitations. In this paper, we applied PBC to pretreat non-uniform backgrounds in thermal images caused by uneven heating. Experimental results showed that our proposed method can significantly improve the SNR of images.

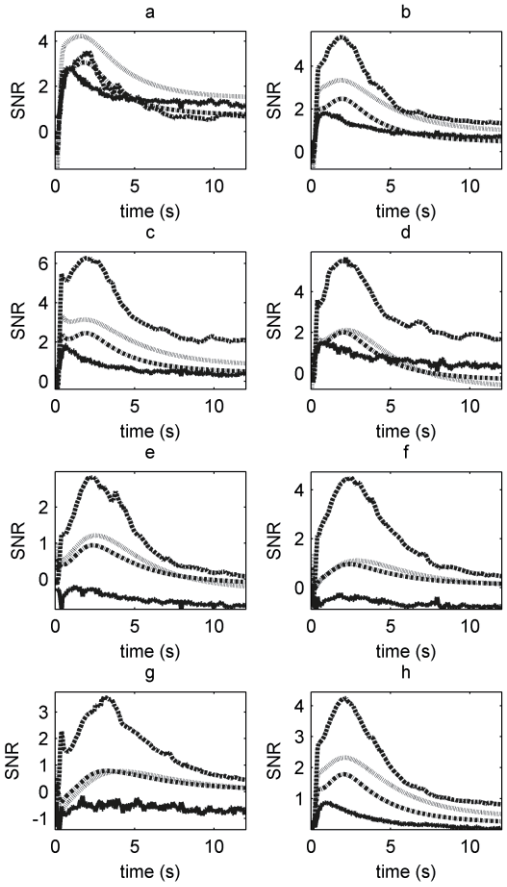

Figure 6. The SNR of thermal images under different pretreatments methods (I. TSR, II. WS, III. PBC) for defective regions A (a), B (b), C (c), D (d), E (e), F (f), G (g) and whole defect regions (h) (solid line: no pretreatment, dot dash line: I, dot line: I+II, dash line: I+II+III).

References

[1] A. Reh, et al.: "Porosity Maps - Interactive Exploration and Visual Analysis of Porosity in Carbon Fiber Reinforced Polymers" *Computer Graphics Forum*, vol.31, no.3pt3, pp.1185-1194, 2012.

[2] C. Maierhofer, et al.: "Quantitative impulse thermography as non-destructive testing method in civil engineering – Experimental results and numerical simsimulations, "*Construction And Building Materials*, vol.19, no.10, pp.731-737, 2005.

[3] N. Akhter, et al.: "Location of delamination in laminated composite plates by pulsed laser holography," *Optics And Lasers In Engineering*, vol.47, no.5, pp.584-588, 2009.

[4] C. Ibarra-Castanedo, et al.: "Comparative Study of Active Thermography Techniques for the Nondestructive Evaluation of Honeycomb Structures," *Research In Nondestructive Evaluation*, vol.20, no.1, pp.1-31, 2009.

[5] M. A. Omar, et al.: "A quantitative review of three flash thermography processing routines," *Infrared Physics & Technology*, vol.51, no.4, pp.300-306, 2008.

[6] S. M. Shepard: "Reconstruction and enhancement of active thermographic image sequences," *Optical Engineering*, vol.42, no.5, pp.1337, 2003.

[7] M. S. Benmoussat, et al.: "Automatic metal parts inspection: Use of thermographic images and anomaly detection algorithms, "*Infrared Physics & Technology*, vol.61, pp.68-80, 2013.

[8] R. Hidalgo-Gato, et al.: "Quantification by Signal to Noise Ratio of Active Infrared Thermography Data Processing Techniques," *Optics and Photonics Journal*, vol.03, no.04, pp.20-26, 2013.

[9] F. Gan, et al.: "Baseline correction by improved iterative polynomial fitting with automatic threshold," *Chemometrics and Intelligent Laboratory Systems*, vol.82, no.1-2, pp.59-65, 2006.

[10] W. Ecke, et al.: "Pulsed thermographic inspection of CFRP structures: experimental results and image analysis tools," *International Society for Optics and Photonics*, vol. 9062, pp.F1- F14 , 2014.

[11] P. H. Eilers: "A perfect smoother," *Analytical Chemistry*, vol.75, no.14, pp.3631-3636, 2003.

[12] J. C. Domínguez, et al.: "Chemorheological study of a polyfurfuryl alcohol resin system Pre-gel curing stage," *Industrial Crops And Products*, vol.52, no.321-328, 2014.

[13] U. Braun, et al.: "Influence of the oxidation state of phosphorus on the decomposition and fire behaviour of flame-retarded epoxy resin composites," *Polymer*, vol.4, no.26, pp.8495-8508, 2006.